



AIAS 2017 International Conference on Stress Analysis, AIAS 2017, 6–9 September 2017, Pisa, Italy

Implicit gradient approach for numerical analysis of laser welded joints

Paolo Livieri*, Roberto Tovo

Dept of Engineering, University of Ferrara, via Saragat 1, 44122, Ferrara, Italy

Abstract

This paper analyzes the fatigue strength of laser welded steel joints by applying the implied gradient method. This method is adopted using the same procedure proposed for studying arc welded joints. The fatigue scatter band of laser joints, obtained from numerical analysis of experimental data taken from the literature, is different from the relative curve of arc welded joints. However, at high cycles fatigue the two bands maintain exactly the same average values and the same scatter. The fatigue strength of lap joints with different weld patterns confirms the use of the proposed generalized fatigue scatter band for laser joints.

Copyright © 2018 The Authors. Published by Elsevier B.V.

Peer-review under responsibility of the Scientific Committee of AIAS 2017 International Conference on Stress Analysis

Keywords: laser weld; fatigue; welded joints; implicit gradient

1. Introduction

The idealization of a weld considers an open notch with a linear flank and a null notch tip radius [Lazzarin and Tovo (1997), Livieri and Lazzarin (2005)]. Therefore, the stress field in the neighborhood of the notch tip has to be considered as singular [Williams (1952)] and the assessment of the fatigue strength of complex welded structures can be carried out by using the numerical design methods classified in scientific literature as local methods. The basic idea of these approaches is to consider the value of an effective physical quantity related to the stress field around the area where the fatigue crack will nucleate [Radaj and Sonsino (1998), Lazzarin and Zambardi (2001), Berto and Lazzarin (2009), Meneghetti (2008), Susmel and Taylor (2011)].

*E-mail address: paolo.livieri@unife.it

The propagation phase, at least in welded specimens used for fatigue testing, is usually negligible when compared to the time required for propagating the crack up to a few millimeters [Sørensen et al. 2006].

The idea that material damage is mainly due to the fatigue behavior of a zone around the notch tip is also considered in the implicit gradient method. This approach has been proposed as a design method for welded arc structures or spot welds without making any difference to the procedure in terms of sheet thickness, joint shape or loading type [Tovo and Livieri (2011)]. Many experimental series, very different in terms of sheet thickness and geometry (for example thickness ranging from 3 mm to 100 mm), were analyzed by means of the implicit gradient approach and obtained a master Woehler curve suitable for the evaluation of the fatigue strength of joints under tensile or bending nominal stress. The procedure offers the advantage of representing welded joints in their three-dimensional form without necessarily performing exemplifications in the shape.

The laser procedure is an alternative choice for connecting thin plates usually employed in the automotive industry [Sonsino et al. (2006)]. Furthermore, laser welded joints are also employed in many industrial sectors using thin plates [Cho et al. (2004)] or plates up to 12 mm [see Frank et al. (2011)]. The standard local approaches used for thick joints are not usually suitable for the assessments of laser welded joints. For instance, the approach of fictitious enlargements of notch tip radii proposed by Raday (1996) for assessing welded joints connecting thin sheets with the notch stress approach, a reference radius of 0.05 mm is usually chosen. [Karakas et al. (2008), Bruder et al. (2012), Baumgartner et al. (2015), Marulo et al. (2017)].

This paper, by means of the implicit gradient method, will examine the fatigue behavior of laser welded steel joints taken from the literature. For lap joints, the thicknesses analyzed are typical of the plates used in the automotive field. The fatigue strength of lap joints with different weld patterns is also analyzed: longitudinal-line segment group pattern (LLSG), ladder pattern, sawtooth pattern and double arc pattern (DCA).

Nomenclature

σ_{eff}	effective stress
σ_{eq}	equivalent stress
σ_{av}	average stress
$\sigma_{\text{eff,max}}$	maximum effective stress
Δ	range
∇^2	Laplace operator
2α	opening angle
c	characteristic length
g	gap between the two plates
FE	finite element
w	width
w_d	length of weld bead
R	nominal load ratio
s	minimum dimension of the mesh elements
t	thickness
d	weld width
N	fatigue life, cycles to failure
V	volume

2. Basic equation

The implicit gradient method defines an effective stress σ_{eff} related to the local stress fields generated from a stress raiser such as a sharp V notch or a weld [Lazzarin and Tovo (1998)]. It is assumed that fatigue damage is due to the

average of stress, evaluated on the whole component, of a physical quantity called equivalent stress σ_{eq} considered as directly linked to fatigue damage [Pijaudier-Cabot and Bažant (1987), Tovo and Livieri (2007-8)]. From a computational point of view, the effective stress σ_{eff} can be calculated, point by point, by solving the Helmholtz differential equation in volume V of the component by imposing Neumann as boundary conditions [Peerlings et al. (1996) and (2001)]:

$$\sigma_{eff} - c^2 \nabla^2 \sigma_{eff} = \sigma_{eq} \quad \text{in } V \quad (1)$$

where c is an intrinsic parameter related to the material and having the physical dimensions of a length, ∇^2 is the Laplace operator and σ_{eq} is the damaging stress. In this work σ_{eq} coincides with the first principal stress evaluated with finite elements for linear elastic material. A non-linear behavior could be introduced without any particular problems [see Tovo et al. (2008 b), Livieri et al. (2016), Novak et al. (2016)] but in the case of a small plastic zone a linear elastic behavior can also be considered in the case of a singular stress field [see Lazzarin and Livieri (2000)].

With reference to figure 1, as a first step in the numerical procedure a classic FE analysis is performed to calculate the stress tensor of Cauchy, followed by a second FE analysis that solves the Helmholtz differential equation Eq. (1) thus obtaining the effective stress σ_{eff} across the joints. The second FE analysis takes advantage of the first one. In the second FE analysis the operator uses exactly the same mesh as the one set up in the first classical stress analysis.

For arc welded joints, in previous works [Tovo-Livieri (2007-8)] the fatigue scatter band was evaluated between 10^4 and $5 \cdot 10^6$ cycles to failure in terms of maximum effective stress variation $\Delta\sigma_{eff, max}$. This scatter band is independent of the geometry of the joints and can be used for the estimation of the safety factor of welded joints. Figure 1 shows the fatigue scatter with a slope equal to 3 for the joint band procedure that can be used for the evaluation of fatigue life if the effective stress σ_{eff} is known. Alternatively, instead of solving the differential equation (1) all over the welded component, it is possible to evaluate the effective stress at the single point of the weld (at the toe or at the root) with a simplified procedure that calculates the value of the weighted average stress σ_{av} and then, through a correlation coefficient, estimates the maximum effective stress $\sigma_{eff, max}$ [Maggiolini et al. (2015)]. Figure 2 shows how the average stress σ_{av} can be correlated with the effective stress σ_{eff} for a sharp V-notch having a small opening angle 2α in comparison with the width of the plate. It is possible to define an average stress in a generic point X as an integral average of an equivalent local stress σ_{eq} , weighted by a Gaussian function $\psi(X, Y)$ depending on the distance h between points X and Y of the body:

$$\sigma_{av}(X) = \frac{1}{V_r(X)} \int_V \psi(X, Y) \sigma_{eq}(Y) dV = \frac{\int_V \psi(X, Y) \sigma_{eq}(Y) dV}{\int_V \psi(X, Y) dV} \quad \text{with} \quad V_r(X) = \int_V \psi(X, Y) dV \quad (2)$$

In Eq. (9) it is possible to use two different weight functions depending on the space dimension of the investigated structural problem. For three dimensional problems:

$$\psi = \frac{e^{-\frac{h^2}{2L^2}}}{(L\sqrt{2\pi})^3} \quad L = c\sqrt{2} \quad \text{3D problem} \quad (3)$$

with h equal to the Euclidian distance between X and Y . In figure 2, X agrees with P .

3. Fatigue analysis of laser welded joints

In laser welded joints, the thermally altered zone is rather limited compared to the traditional arc welding process (see Asim 2011). However, in this paper laser welded joints are analyzed with the implicit gradient approach without altering the methodology previously proposed for arc welds. It was assumed that fatigue damage is due to the maximum principal stress evaluated under linear elastic hypotheses by assuming a value of c equal to 0.2 mm for the material as in the case of welded arc joints.

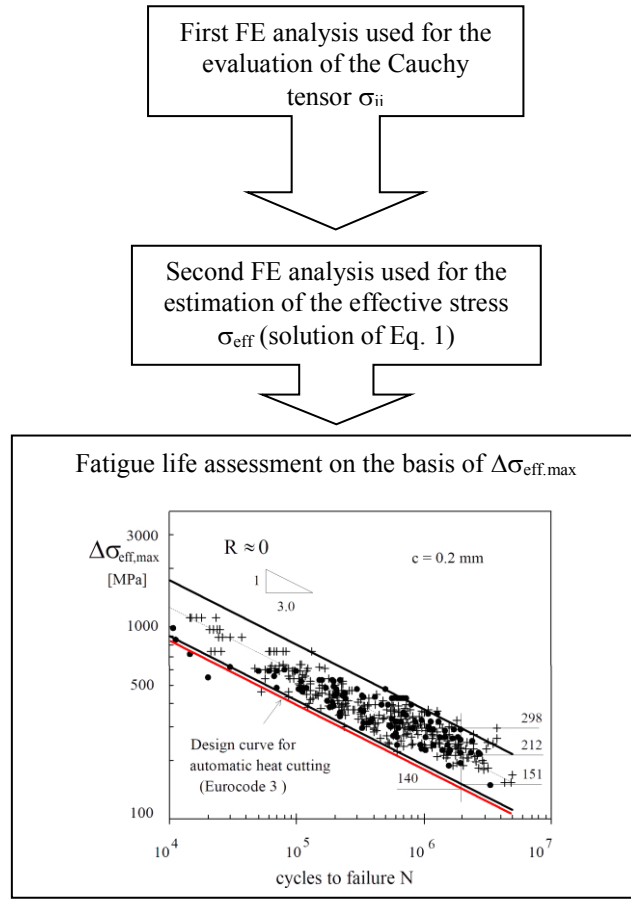


Fig. 1. Reference procedure.

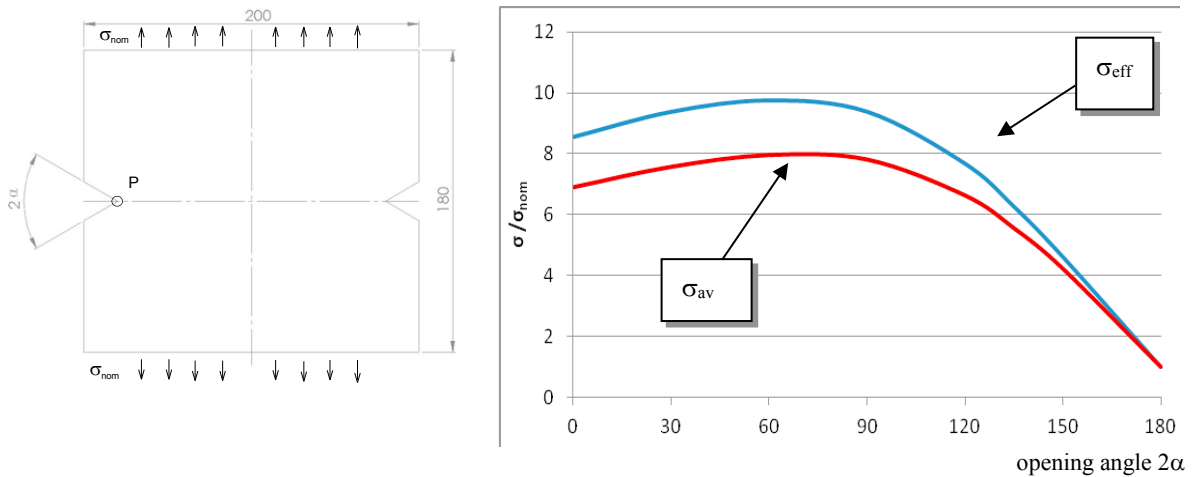


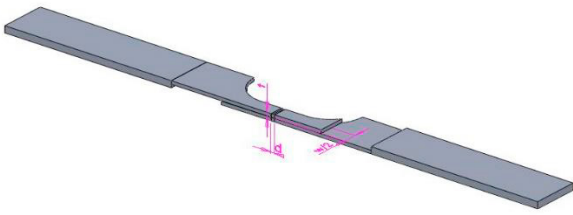
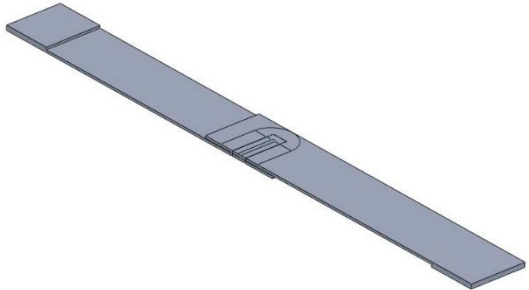
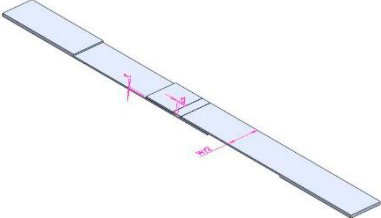
Fig. 2. Relation between the average stress σ_{av} and the effective stress σ_{eff} obtained by solving the implied gradient equation (1) for a plate with a small sharp V-notch [Maggiolini et al. 2015].

3.1. Lap joints

First of all we analyze the fatigue behavior of a lap joint subjected to remote tensile loading. Table 1 summarizes the different geometries of laser joints made of steel into 3 series. The nominal load is a tensile loading for all series. Type A represents a lap joint where the central section has been reduced in width. The welded sheets were machined into specimens with a dog-bone shaped profile. Type B is another lap joint but the bead length is less than the size of the nominal section. In addition, the bead ends has a rounded profile. Type C consists of typical lap joints with the weld extending across the entire width. Figure 3 shows two typical meshes of series A characterized by two different mesh sizes with a different s/t ratio (s is the minimum dimension of the elements and t is the thickness of the sheets). A mesh with a size of $s/t \approx 0.5$, in fact, gives the same numerical results as an accurate mesh with minimum size elements $s/t \approx 0.03$. Although the more detailed mesh is half-thickness, the differences in the calculation of the maximum effective stress $\sigma_{\text{eff,max}}$ relative to the nominal stress ($\sigma_{\text{eff,max}}/\sigma_{\text{nom}}$) ranges from 9.13 to 9.25 with a difference of around 1%. This trend confirms the capability of a fast convergence even in the case of small joints [see Tovo-Livieri (2011)].

The type A welded joints were experimentally analyzed by Asim et al. (2011). All experimental data relate to a single geometry and cover a fatigue life ranging from $6 \cdot 10^3$ cycles to $1.7 \cdot 10^5$ cycles. Type B is composed of 4 sets of data that Wang used to analyze the effect of: thickness, width, weld bead and gap size that can be created between the two welded plates after the welding process. With the implicit gradient method, the gap representation is not a problem because it is necessary to take the three-dimensional CAD model into account (the gap is usually defined as a percentage of the thickness).

Table 1: Lap joint made of steel subjected to nominal tensile loading (half joint)

 <p>$t = 0.93 \text{ mm}, d = 1.0 \text{ mm}, w = 8 \text{ mm}$</p> <p>Type A: material SAE J2340 300Y HSLA [Asim et al. (2011)]</p>	 <p>$t = 0.76 \div 1.78 \text{ mm}, d = 1.2 \div 1.4 \text{ mm}, w = 38.1, w_d = 25.4 \text{ mm}$</p> <p>Type B: material SAE 1005 [Wang (1995)]</p>
 <p>$t = 0.41 \div 2.54 \text{ mm}, d = 0.61 \text{ mm}, w = 38.1$</p> <p>Type C: material AISI 1008 [Albright et al. (1990)]</p>	

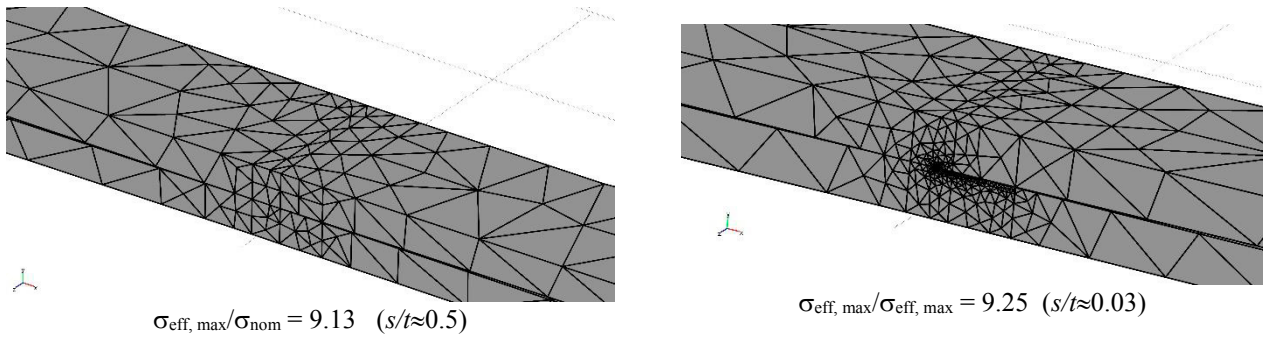


Fig. 3. Example of mesh used in the FE analysis. Maximum value of the effective stress $\sigma_{eff, max}$ as a function of the mesh size (σ_{nom} is the remote tensile stress, s is the size of the smallest element).

Figure 4 shows the fatigue scatter band of laser steel welded joints in terms of maximum effective stress range evaluated by means of the implicit gradient approach described in section 2. The scatter bands are related to mean values plus/minus 2 standard deviations. The slope is different in relation to the scatter bands of arc welded joints. We have a slope of 4.7 instead a slope of 3.0. Table 2 summarizes the characteristic values in terms of effective stress of the two scatter bands for welded joints made of steel.

Table 2. Reference value of the effective stress of the two fatigue scatter bands at $5 \cdot 10^6$ cycles to failure

Weld type	97.70% [MPa]	50% [MPa]	2.30% [MPa]	k
Arc	111	156	219	3.0
Laser	113	157	215	4.7

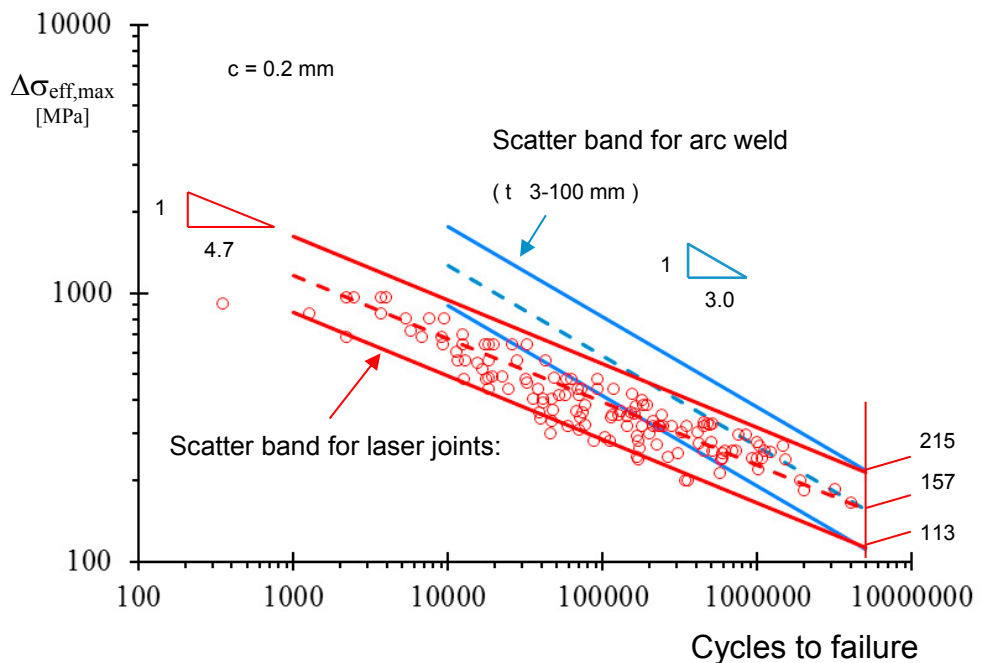


Fig. 4. Scatter band for steel welded joints in terms of maximum effective stress range (scatter bands related to mean values plus/minus 2 standard deviations)

3.2. Effect of weld pattern

In order to consider the increase in fatigue strength of the lap joint, Albright et al. (1990) proposed different types of welded joint configurations. A straight-line lap weld made in a direction perpendicular to the load direction is the simplest laser lap weld for fatigue testing (see table 1). Figure 5 shows four weld patterns very different from the typical lap joint of table 1: *longitudinal-line segment group pattern* (LLSG), *ladder pattern*, *sawtooth pattern* and *double circular arc pattern* (DCA). The thickness was of 0.61 mm for all specimens with an overlap of 25.4 mm and a width of 38.1 mm.

As an example, figure 6 reports a typical mesh used in the analysis of a lap joint for the case of the longitudinal-line segment group pattern. For each case a first FE analysis with a raw mesh was used to identify the critical points, then a second FE analysis with a fine mesh was optimized only in the weld zone where the effective stress reaches its maximum value. Furthermore, in order to reduce the number of elements used in the numerical analysis, a plate with a reduced width was considered. On the basis of recent studies about the fatigue strength of arc welds (see Livieri-Tovo 2017) the reduction of the width may result in a change in maximum effective stress. The trend of the stress along the weld depends on the ratio between the thickness and the width of the specimen, but this aspect will be considered in our next paper.

Table 3 shows the results of the numerical analysis of the joints in figure 5. The numerical results were obtained after careful convergence analysis. Table 3 reports the stress concentration factor K_t for the different welded joints defined as:

$$K_t = \frac{\sigma_{\max, eff}}{\sigma_{nom}} \quad (4)$$

Finally, the fatigue strength of lap joints is reported in figure 7. In terms of maximum effective stress the experimental points fall into the fatigue scatter band of laser joints proposed in figure 5.

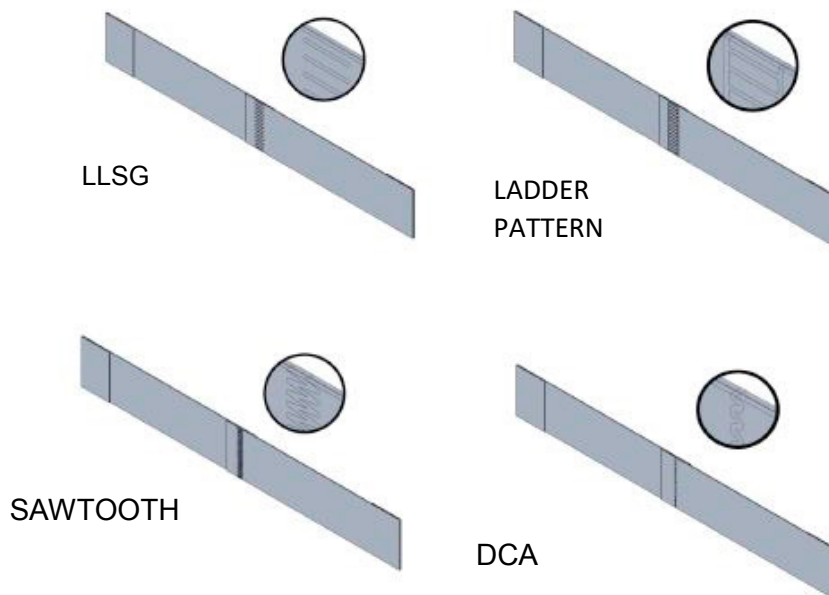


Fig. 5. Different types of lap joints. The thickness of the plates was of 0.61 mm (for geometrical details see Albright et al. 1990)

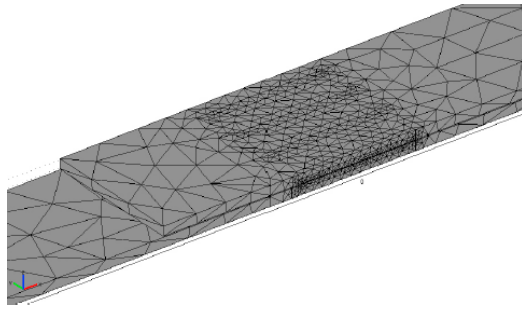






Fig. 6. Example of mesh used in the FE analysis of a longitudinal-line segment group pattern. The thickness of the plates was of 0.61 mm (for geometrical details see Albright et al. 1990)

Table 3. Stress concentration factor K_t for different types of lap joints

				
	LLSG	LADDER PATTERN	SAWTOOTH	DCA
K_t	2.8	2.2	2.4	2.6

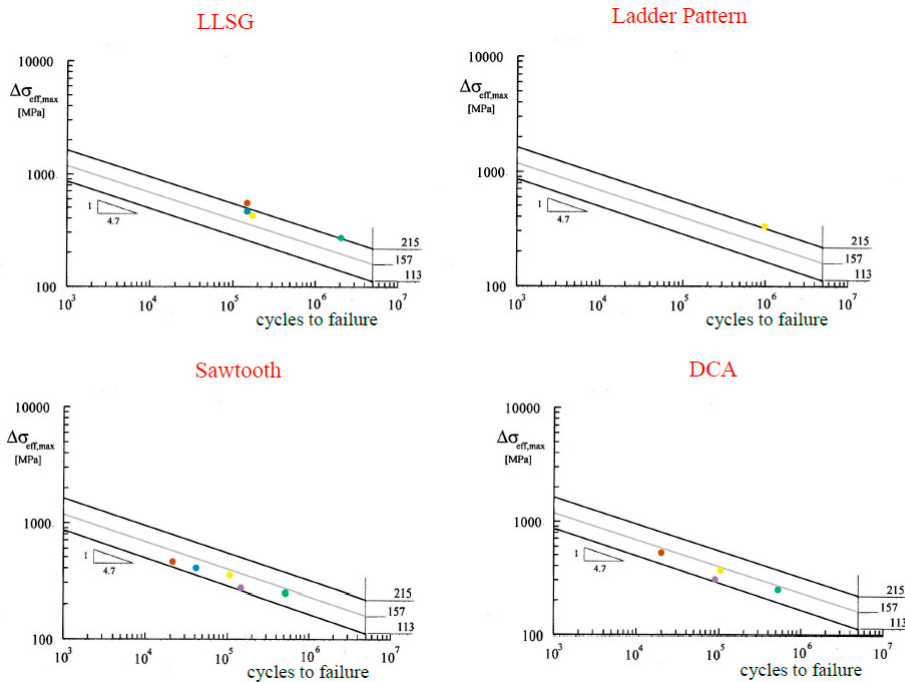


Fig. 7. Fatigue life of different types of lap joints in terms of the range of maximum effective stress by using the fatigue scatter band of figure 6. The thickness of the plates was 0.61 mm

4. Conclusions

The implicit gradient method could analyze the fatigue behavior of the laser welded steel joints by means of three-dimensional FE analysis. For a medium and low number of cycles, the laser weld shows a greater slope of the Woehler curve. However, at high cycles fatigue the effective stress does not depend on the welding technology. For fatigue life at 5 million cycles and a survival probability of 50%, an effective stress value of about 160 MPa seems to be a common threshold for the various types of steel welds also with a complex weld bead profile.

References

- Albright C.E., Hsu C., Lund R.O., 1990. Fatigue strength of laser-welded lap joints. *Journal of laser applications*, pp. 26–32
- Asim K., Sripichai K, Pan J., 2011. Fatigue Failure of laser welds in Lap-Shear Specimens of High Strength low alloy (HSLA) steels under cyclic loadings conditions. *SAE 2011-01-0473*, 4 (1), pp. 571–580
- Baumgartner J., Schmidt H., Ince E., Melz T., Dilger K., 2015. Fatigue assessment of welded joints using stress averaging and critical distance approaches. *Welding in the World*, Vol. 59 (5), pp. 731–742
- Berto F., Lazzarin P., 2009. A review of the volume-based strain energy density approach applied to V-notches and welded structures, *Theoretical and Applied Fracture Mechanics*, 52-3, pp. 183–194
- Bruder T., Störzel K., J. Baumgartner, Hanselka H., 2012, *International Journal of Fatigue* 34, pp. 86–102
- Cho S.-K., Yang Y.-S., Son K.-J., Kim J.-Y., 2004. Fatigue strength in laser welding of the lap joint. *Fin. Elem. Analysis and Des.* 40, 1059–1070
- Frank D., Remes H., Romanoff J., 2011. Fatigue assessment of laser stake-welded T-joints, *International Journal of Fatigue* 33, 102–114
- Karakas Ö., Morgenstern C., Sonsino C.M., 2008. Fatigue design of welded joints from the wrought magnesium alloy AZ31 by the local stress concept with the fictitious notch radii of $r_f=1.0$ and 0.05 mm, *International Journal of Fatigue*, 30-12, pp. 2210–2219
- Lazzarin P., Livieri P., 2000. Welded joints: limits on criteria for plasticity zones located at weld toes, *Welding International*, 14-10, pp. 806–810
- Lazzarin P., Tovo R., 1998. A Notch Intensity Approach to the Stress Analysis of Welds. *Fatigue and Fracture of Engineering Materials and Structures* 21, pp. 1089–1104
- Lazzarin P., Zambardi R., 2001. A finite-volume-energy based approach to predict the static and fatigue behavior of components with sharp V-shaped notches. *Int J Fract*;112:275–98
- Livieri P., Lazzarin P., 2005. Fatigue strength of steel and aluminium welded joints based on generalised stress intensity factors and local strain energy values, *International Journal of Fracture*, 133, pp. 247–376
- Livieri P., Salvati E., Tovo R., 2016. A non-linear model for the fatigue assessment of notched components under fatigue loadings. *International Journal of Fatigue*, Vol. 82-3, pp. 624–633
- Livieri P., Tovo R., 2017. Analysis of the thickness effect in thin steel welded structures under uniaxial fatigue loading. *International Journal of Fatigue*, Vol. 101-2, pp. 363–370
- Maggiolini E., Livieri P., Tovo R., 2015. Implicit gradient and integral average effective stresses: Relationships and numerical approximations, *Fatigue & Fracture of Engineering Materials & Structures*, Vol. 38-2, pp. 190–19
- Marulo G., Baumgartner J., Frenzo F., 2017. Fatigue strength assessment of laser welded thin-walled joints made of mild and high strength steel, *International Journal of Fatigue* 96, pp. 142–151
- Meneghetti G., 2008. The Peak Stress Method Applied To Fatigue Assessments Of Steel And Aluminium Fillet-Welded Joints Subjected To Mode I Loading *Fatigue & Fracture of Engineering Materials & Structures* 31-5, pp: 346–369
- Novak, J.S., Benasciutti, D., De Bona, F., Stanojević, A., De Luca, A., Raffaglio, Y., 2016. Estimation of material parameters in nonlinear hardening plasticity models and strain life curves for CuAg alloy. *IOP Conference Series: Materials Science and Engineering* 119(1),012020
- Pijaudier-Cabot G., Bažant Z.P., 1987. Nonlocal Damage Theory, *Journal of Engineering Mechanics*, 10, pp. 1512–1533.
- Peerlings R.H.J., de Borst R., Brekelmans W.A.M., de Vree J.H.P., 1996. Gradient enhanced damage for quasi-brittle material. *International Journal of Numerical Methods in Engineering* 39, pp. 3391–3403.
- Peerlings R.H.J., Geers M.G.D., de Borst R., Brekelmans W.A.M. 2001. A critical comparison of nonlocal and gradient-enhanced softening continua. *International Journal of Solids and Structures*, 38, pp. 7723–7746
- Radaj D., 1996. Review of fatigue strength assessment of nonwelded and welded structures based on local parameters, *International Journal of Fatigue*, Vol. 18-3, pp. 153–170
- Radaj, D., Sonsino, C.M. (1998). *Fatigue assessment of welded joints by local approaches*, Abington Publishing, Abington, Cambridge.
- Sonsino C.M., Kueppers M., Eibl M., Zhang G., 2006. Fatigue strength of laser beam welded thin steel structures under multiaxial loading *International Journal of Fatigue*, Volume 28, Issues 5–6, 2006, pp. 657–662
- Sørensen J.D., Tychsen J., Andersen J.U., Brandstrup R.D., 2006. Fatigue Analysis of Load-Carrying Fillet Welds *Journal of Offshore Mechanics and Arctic Engineering*, Vol. 128, pp. 65–74
- Susmel L., Taylor D., 2011. The Theory of Critical Distances to estimate lifetime of notched components subjected to variable amplitude uniaxial fatigue loading, *International Journal of Fatigue*, Vol. 33, 7, 900–911
- Tovo R., Livieri P., 2007. An implicit gradient application to fatigue of sharp notches and weldments. *Eng. Fract. Mech.*, 74, pp. 515–526
- Tovo R., Livieri P., 2008. An implicit gradient application to fatigue of complex structures, *Eng. Fract. Mech.*, 75 (7), pp. 1804–1814
- Tovo R., Livieri P., Capetta S., 2008 b. Gradiente implicito e non linearita' del materiale, XXXVII AIAS, 10–13 Settembre 2008, pp. 383–384
- Tovo R., Livieri P., 2011. A numerical approach to fatigue assessment of spot weld joints. *Fatigue and Fracture of Engineering Materials and Structures*, Vol. 34-1, pp. 32–45
- Wang P.C., 1995. Fracture mechanics parameter for the fatigue resistance of laser welds, *International Journal of Fatigue*, Vol. 17-1, pp. 25–34
- Williams M.L. 1952, Stress singularities resulting from various boundary conditions in angular corners of plates in extension. *Journal of Applied Mechanics*:19, pp. 526–528.